OPEN

DNA methyltransferase inhibitor 5-azacytidine enhances neuroblastoma cell lysis by an oncolytic parainfluenza virus

Kritika Kedarinath, Elisabeth M. Shiffer and Griffith D. Parks

Studies with neuroblastoma have shown that the presence of aberrant DNA epigenetic modifications mediated by DNA methyltransferases correlates with poor prognosis, making these enzymes a target for therapeutics based on synthetic epigenetic modulators such as DNA methyltransferase inhibitors (DNMTi). Here, we have used a neuroblastoma cell line model to test the hypothesis that treatment with a DNMTi would enhance cell killing when used in combination with oncolytic Parainfluenza virus 5 (P/V virus), a cytoplasmic-replicating RNA virus. Pretreatment of SK-N-AS cells with the DNMTi 5-azacytidine substantially enhanced P/V virus-mediated cell death in a dose- and multiplicity of infection-dependent manner. Infection with the virus alone and the combination treatment with 5-azacytidine and P/V virus infection led to the activation of caspases-8, -9, and -3/7. Inhibition of caspases using a pan-caspase inhibitor minimally affected cell killing by P/V virus alone, but by contrast, largely reduced cell death mediated by 5-azacytidine treatment alone or in combination with P/V virus infection. 5-Azacytidine pretreatment dampened P/V virus gene expression and growth within the SK-N-AS cell population, which correlated with enhanced expression of important antiviral genes such as interferon-β and *OAS2*. Taken together, our data support the role of combination treatment using 5-azacytidine and an oncolytic P/V virus for neuroblastoma therapy. *Anti-Cancer Drugs* 34: 916–928 Copyright © 2023 The Author(s). Published by Wolters Kluwer Health, Inc.

Anti-Cancer Drugs 2023, **34**:916–928

Keywords: DNA methyltransferase inhibitors, neuroblastoma, oncolytic virus

University of Central Florida, College of Medicine, Orlando, Florida, USA

Correspondence to Griffith D. Parks, PhD, Burnett School of Biomedical Sciences, University of Central Florida, College of Medicine, Orlando, FL 32827, USA
Tel: +1 (407) 266 7011; e-mail: griffith.parks@ucf.edu

Received 15 March 2023 **Revised form accepted** 12 April 2023.

Introduction

Neuroblastoma is an extracranial paediatric cancer that typically originates from immature nerve cells, commonly forming in either adrenal glands or along the sympathetic nervous system [1]. As the second most common childhood cancer, neuroblastoma comprises ~6% of all paediatric cancers, however, it accounts for a disproportionately high death rate of ~15% [2]. A small subset of neuroblastoma tumours spontaneously undergoes regression, while a larger subset of tumours will progress into aggressive, high-risk cases. As high-risk neuroblastoma tumours do not respond well to conventional cancer treatment such as radiation and chemotherapy, there is an urgent need to address the limited therapeutic options for neuroblastoma.

Aberrant DNA epigenetic modifications, particularly mediated by enzymes responsible for DNA methylation, have shown to be attractive therapeutic targets for high-risk cancers [3]. DNA methyltransferases (DNMT1, DNMT3A, DNMT3b, and DNMT3L) are responsible for establishing methylation patterns in chromosomal DNA, thereby leading to the stable repression of various genes [3]. Studies have shown that expression of DNMTs is modulated during the emergence of neuroblastoma, particularly in the case of DNMT3A and DNMT3B. These enzymes can be over-expressed in high-risk neuroblastoma tumours and in tumours that are resistant to chemotherapy treatment with the DNA-damaging agent cisplatin [4]. Due to the correlation between abnormal methylation patterns and poor prognosis in neuroblastoma patients, the use of DNMT inhibitors (DNMTi) to target these epigenetic aberrations is of high interest.

DNMTi 5-azacytidine has shown great efficiency against myelodysplastic syndromes and other solid tumours [5–7]; however, this synthetic epigenetic modulator is yet to be extensively characterized in an in-vitro neuroblastoma model.

Oncolytic viruses are an emerging cancer treatment that has been extensively studied and characterized in various tumour types [8,9]. They have gained interest since the approval of a genetically modified HSV-1 IMLYGIC (Talimogene Laherparepvec), to treat melanoma patients [10,11]. A number of negative strand RNA viruses from the *Paramyxoviridae* family, such as the Newcastle Disease virus, mumps virus, and measles virus have been developed as potential oncolytic virus candidates [12–17]. The P/V gene of the paramyxovirus

 DOI: 10.1097/CAD.0000000000001525

wild type parainfluenza virus 5 (WT PIV5) encodes the phosphoprotein P which is an essential subunit of the viral RNA dependent RNA polymerase, and V protein, which plays roles in blocking both type I interferon (IFN-I) induction as well as signalling by directing the degradation of signal transducer and activator of transcription 1 (STAT1) [18]. The introduction of six nucleic acid substitutions in the viral P/V gene converts non-cytopathic WT PIV5 into cytopathic P/V mutant virus [Parainfluenza virus 5 (P/V virus)] [19] which induces cytopathic effects in tumour cells, upregulates double-stranded RNA (dsRNA)-mediated IFN-I pathways, and causes shutoff of host and viral translation through protein kinase R (PKR) pathways [20,21]. In addition to this, the P/V virus has shown properties of an oncolytic virus in mouse model systems [22].

We have previously shown that treatment of lung carcinoma cells with chemical epigenetic modulators such as histone deacetylase (HDAC) inhibitors can enhance P/V virus-mediated killing by upregulating caspase activity [23]. Given these prior studies and the intense interest in combination therapies for neuroblastomas, we have used an SK-N-AS neuroblastoma cell line model to test the hypothesis that a synthetic DNMTi can also improve neuroblastoma cell killing when used in combination with P/V virus infection.

Materials and methods

Cell lines, viruses, infections, and plaque assays

SK-N-AS cells were kindly provided by T. J. Westmoreland and K. Alexander (Nemours Children's Health, Orlando, Florida, USA). CV-1, A549, SK-N-SH, and Vero cells were procured from ATCC (American Type Culture Collection, Manassas, Virginia, USA). Cultures of SK-N-AS, SK-N-SH, CV-1, Vero, and A549 cells were maintained and grown with Dulbecco's modified Eagle medium (DMEM) supplemented with 10% heat-inactivated foetal calf serum (HI FBS, Gibco, Thermo Fisher Scientific, Waltham, Massachusetts, USA). SK-N-AS and SK-N-SH cells expressing a red nuclear fluorescent protein were generated by transduction with Nuc-Light-Red (NLR) lentivirus purchased from IncuCyte (Sartorius, Bohemia, New York, USA). The resulting NLR cells were cultured in DMEM supplemented with 10% FBS and 0.5 μg/ml puromycin (Invivogen, San Diego, California, USA). HEK-Blue IFN-α/β indicator cells (Invivogen) were maintained as described by K.K and G.D.P. [24].

The PIV5 virus PIV5-P/V-CPI– (P/V virus) expressing green fluorescence protein (GFP) was generated, grown, and tittered in Vero cells as described previously [19,25]. For infections, cells were either mock-infected or infected with virus diluted in DMEM supplemented with 10% BSA (Gibco) as described previously [24,25].

Chemical preparation and treatment

5-Azacytidine and pan-caspase inhibitor Z-VAD-FMK were procured from Millipore Sigma (Burlington, Massachusetts, USA) and Invivogen respectively. They were reconstituted in sterile dimethyl sulfoxide (DMSO) as per manufacturer's instructions. Cells were seeded in appropriate plate formats and treated with either DMSO (vehicle control) or indicated chemical, diluted in DMEM supplemented in 2% HI FBS, as described in figure legends.

Cell viability, cytotoxicity, and caspase assays

Cell viability assays were carried out using the IncuCyte instrument (Sartorius) as previously described [26,27]. Briefly, SK-N-AS NLR cells were plated in triplicate in 96-well plates (Falcon, Corning, New York, USA) at 7000 cells per well and treated as indicated in figure legends. Plates were then incubated in the IncuCyte CO_2 incubator for ~4 days, while images were captured every 6 h using 10× objective in red and phase channels. Red object count (ROC) per well was calculated using IncuCyte software and scans were normalized to the value at time 0 (ROC^{t0}) when treatment or infection was performed.

Cytotoxicity assays were performed using CytoTox-Glo assay (Promega, Madison, Wisconsin, USA), as per manufacturer's instructions. Cytotoxicity or maximum cell lysis was calculated as described previously [26].

For caspase assays, SK-N-AS cells were seeded in white 96-well plates (Corning) at 5000 cells per well. Cells were treated as indicated in figure legends and Caspase-Glo-8, Caspase-Glo-9, and Caspase-Glo-3/7 Assay systems (Promega) were performed as per the manufacturer's instructions. Luminescence readings were recorded 90 min post-addition of the reagent.

Quantification and visualization of infected cells

Cells were cultured in 24-well plates and treated as described in figure legends. Cells were trypsinized, quenched in DMEM supplemented with HI FBS, and subsequently washed with PBS. Flow cytometry was performed using CytoFLEX LX (Beckman Coulter, Brea, California, USA), and 10 000 independent events were recorded. Results were analyzed using CytExpert software (Version 2.4.0.28, Beckman Coulter) to obtain percentage of infected cells and mean fluorescence intensity (MFI) of intact cells.

To visualize virus-infected cells, infection media was replaced with PBS, and images were captured using Zeiss Axiovert fluorescence microscope under a 10× lens (Carl Zeiss Microscopy, LLC, White Plains, New York, USA). Exposure time for phase was 46 ms and fluorescence was 1 s.

Reverse transcription and real-time PCR

Six-well dishes were treated as described in the figure legends, and RNA extraction was performed

using TRIzol (Invitrogen, Thermo Fisher Scientific) as described previously [25]. TaqMan Reverse Transcription Reagents (Applied Biosystems, Foster City, California, USA) were utilized to generate cDNA from 1 µg of total RNA (as per the manufacturer's instructions). Bio-Rad CFX Connect Real-Time and Fast SYBR FAST Green Master Mix (Applied Biosystems) were used to perform quantitative real-time PCR. Relative gene expression was determined using CFX Manager 3.1 Software (Bio-Rad, Hercules, California, USA). Primer sequences for genes *IFN-β*, *OAS2*, and *GAPDH* were as described [25].

IFN-I detection assay

Supernatant from treated cells was collected at the indicated time points and virus was inactivated by acid treatment followed by neutralization, as previously described [24]. HEK-Blue IFN-α/β indicator cells (Invivogen) and QUANTI-Blue reagent (Invivogen), were utilized to detect biological levels of IFN-I as per manufacturer's instructions [24].

Statistics

Mean values and SDs were calculated using GraphPad Prism software (Boston, Massachusetts). *P* values were generated using two-way analysis of variance. In all figures, *, **, and *** indicate *P* values <0.033, <0.002, and <0.001, respectively (*P* value style was set to APA). Graphs for data sets were generated using GraphPad Prism software.

Results

Dose- and multiplicity of infection-dependent enhancement of cell killing of neuroblastoma cells by combined treatment with 5-azacytidine and Parainfluenza virus 5 infection

To monitor the kinetics of cell viability following virus infection, we utilized the IncuCyte instrument for real-time monitoring of cell numbers [26]. In this assay, SK-N-AS cells that stably express a nuclear red fluorescent protein (SK-N-AS NLR cells) are used to enable the IncuCyte fluorescence detectors to count intact cell numbers. ROC per field is calculated every 6 h and expressed as remaining ROC normalized to the initial scan at time 0 (ROC^{t0}) at the time of virus addition (ROC/ROC^{t0}) (Fig. 1b–e).

We determined the kinetics of loss of SK-N-AS NLR cell viability after the combination treatment with DNMTi 5-azacytidine and P/V virus infection. SK-N-AS NLR cells were pretreated overnight with DMSO as a vehicular control or with increasing doses of 5-azacytidine [5,6]. Cells were then mock-infected or infected with P/V virus at a multiplicity of infection (MOI) of 10 plaque forming units (PFU)/cell, and subsequently cultured with either DMSO or 5-azacytidine at the indicated doses. Figure 1a shows representative fluorescence images of DMSO- or 5-azacytidine-treated SK-N-AS NLR cells that were captured at 0 and 30 h post-infection (hpi) after mock or P/V virus infection. The images show red nuclei (ROC) of the SK-N-AS NLR cells and 30 hpi images additionally show green fluorescence derived from the GFP expressed by P/V virus infection. Most importantly, there is a clear loss of ROC in cells treated with a combination of 5-azacytidine and P/V virus infection compared to control-treated cells.

As seen in Fig. 1b, mock-infected cells that were pretreated with DMSO continued to proliferate over time (blue curve), with an increase of ROC up to 200% by ~36 hpi. By contrast, cells infected with the P/V virus showed a decrease in ROC over time, reaching 50% of time 0 by ~48 hpi, (indicated by the dotted line in the figure) (red curve; Fig. 1b). When pretreated with 5-azacytidine, mock-infected cells showed a dose-dependent decrease in ROC reaching 50% of time 0 at ~24 hpi at a dose of 10 µM (blue curves, Fig. 1c–e). By contrast, Fig. 1c–e shows that P/V virus-infected cells pretreated with 1, 5, and 10 µM 5-azacytidine (red curves) had enhanced loss of ROC reaching 50% of time 0 at ~42, 30, and 24 hpi, respectively. Together, these data demonstrate that pretreatment with 5-azacytidine leads to increased cell killing following infection with P/V virus.

To determine if the MOI of P/V virus alters the kinetics of cell killing, SK-N-AS NLR cells were pretreated with either DMSO (Fig. 2a) or 5 µM 5-azacytidine (Fig. 2b) overnight. Pretreated cells were then mock-infected or infected with the P/V virus at increasing MOIs of 0.1, 1, and 10 PFU/cell and then supplemented with DMSO or 5 µM 5-azacytidine. ROC was recorded every 6 h. As shown in Fig. 2a, P/V virus-infected cells pretreated with DMSO showed a reduction in ROC in an MOI-dependent manner, reaching 50% of time 0 at ~45 and ~63 hpi for MOIs of 10 and 1 PFU/cell (purple and green lines, respectively). In Fig. 2b, the ability of 5-azacytidine pretreatment to enhance P/V virus killing was also MOI-dependent, but the loss of ROC reached 50% of time 0 more rapidly – ~35, ~48 and ~66 hpi for MOI of 10 (purple curve), 1 (green curve) and 0.1 PFU/cell (red curve), respectively.

Taken together, these data indicate that the combination of 5-azacytidine treatment and P/V virus infection robustly reduces neuroblastoma cell viability in a dose- and MOI-dependent manner. For subsequent experiments shown below, we performed pretreatment of cells with 5 µM 5-azacytidine in combination with P/V virus infections at MOI of 10 PFU/cell, due to the optimal effectiveness of reducing cell viability of P/V infected cells compared to levels of basal toxicity.

Fig. 1

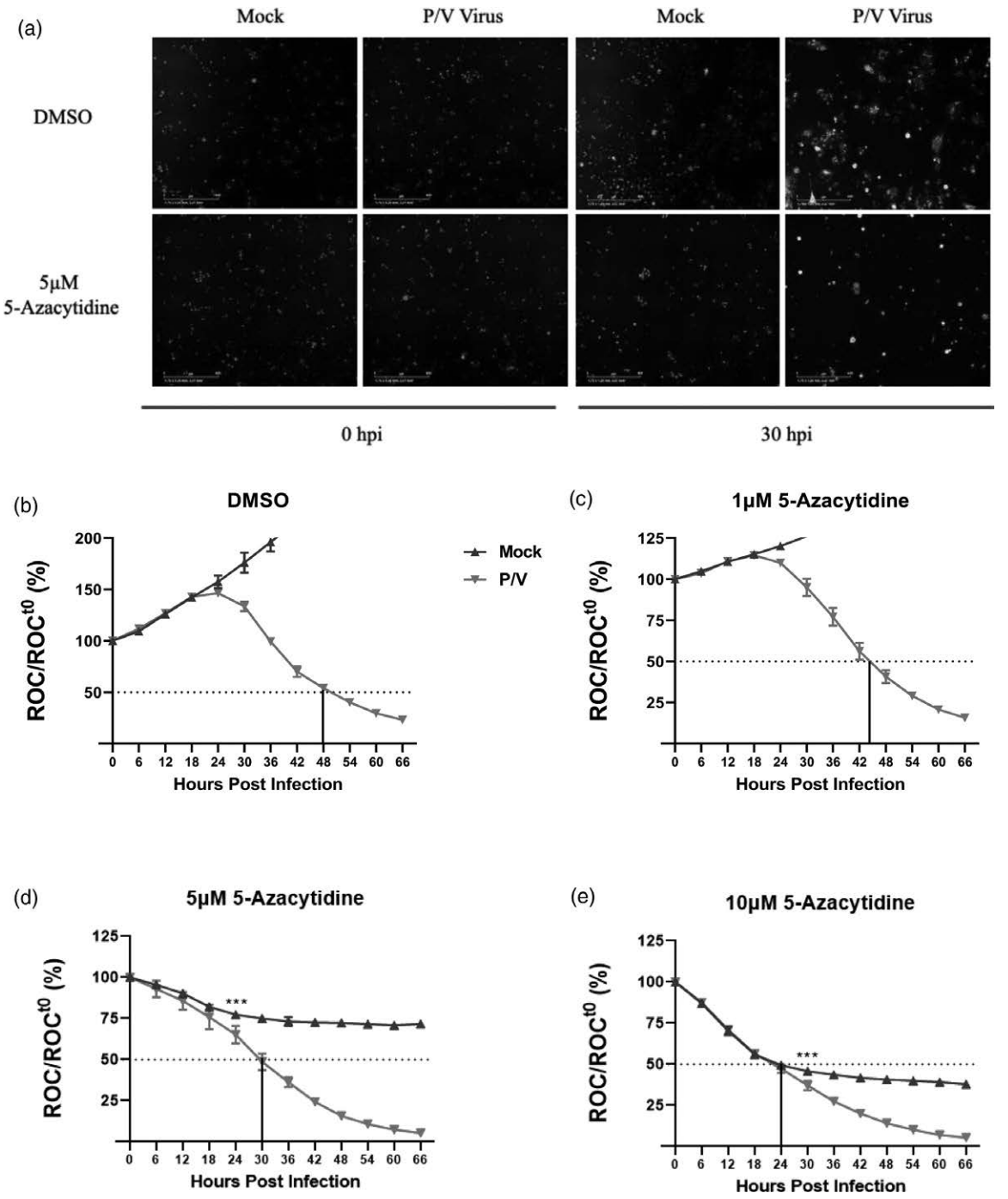

Enhanced killing of neuroblastoma cells by combination treatment with DNMT inhibitor 5-azacytidine and P/V virus infection. SK-N-AS cells expressing nuclear red fluorescent protein (SK-N-AS NLR cells) were pretreated with either (b) DMSO as vehicular control, or with 1, 5, or 10 μM 5-azacytidine (c–e respectively) for ~19 h. Cells were mock-infected or infected with P/V virus at an MOI of 10 PFU/cell and cultured in the presence of indicated drug concentration. Red object count (ROC) was recorded in real-time via the IncuCyte system every 6 h by quantifying the number of cells with intact nuclear red fluorescent protein expression. ROC per well was calculated and normalized to ROC at time 0 (ROC^{t0}) when the infection was performed. Values were expressed as percentage of time 0 and are the mean of three replicates with error bars representing SD. *** indicates the point where *P* value <0.001 first begins when comparing virus-infected to mock-infected samples, and this statistical significance extends for later timepoints. The vertical line in each graph indicates the time taken to achieve a 50% reduction in ROC relative to time 0. (a) shows representative fluorescence images taken by the IncuCyte detector at 0 and 30 hpi showcasing cells expressing red nuclei (ROC) and P/V virus-infected cells (GFP). DNMT, DNA methyltransferase; GFP, green fluorescence protein; hpi, hours post-infection; MOI, multiplicity of infection; NLR, Nuc-Light-Red; P/V virus, Parainfluenza virus 5.

Fig. 2

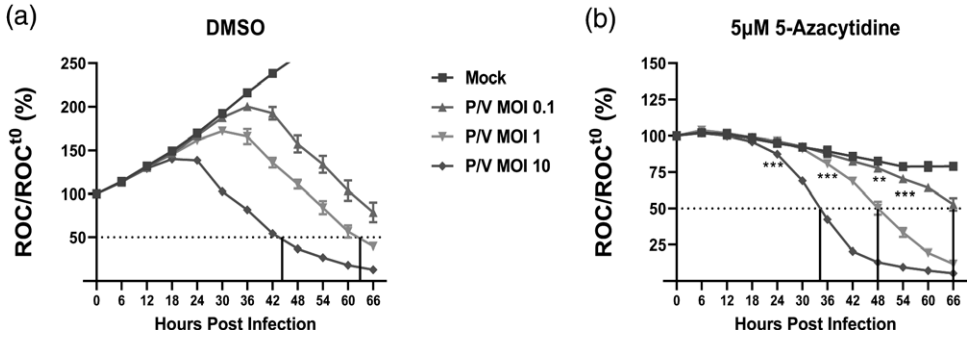

Enhanced killing of neuroblastoma cells with combination pretreatment of 5-azacytidine and P/V virus infection is MOI dependent. SK-N-AS NLR cells were pretreated with (a) DMSO or (b) 5 μM 5-azacytidine for ~19 h. Cells were either mock-infected or infected with the P/V virus at increasing MOIs of 0.1, 1, and 10 PFU/cell and cultured in the presence of indicated drug concentration. ROC per well was normalized to ROC at time 0 (ROC^{t0}) when infection was initiated, as described in Fig. 1. Values are the mean of three replicates with error bars representing SD. ** and *** indicate the point where *P* values <0.002 or <0.001 respectively, first begin when comparing virus-infected to mock-infected samples, and this statistical significance extends for later timepoints. DMSO, dimethyl sulfoxide; MOI, multiplicity of infection. NLR, Nuc-Light-Red; P/V virus, Parainfluenza virus 5; ROC, red object count.

Killing of neuroblastoma cells by Parainfluenza virus 5 alone and in combination with 5-azacytidine differs in the dependence on caspase activity

To directly measure cytotoxicity mediated by combined 5-azacytidine treatment and P/V virus infection, SK-N-AS cells were pretreated with DMSO or 5 μM 5-azacytidine overnight. Pretreated cells were infected with P/V virus at an MOI 10 PFU/cell and then supplemented with DMSO or 5 μM 5-azacytidine. At 30 hpi, cytotoxicity was measured using CytoTox-Glo assay, as described in Materials and Methods. P/V virus infection alone induced ~15–18% of maximal cytotoxicity, and this was increased to ~35% by combination with 5-azacytidine treatment (Fig. 3a). It is noteworthy that drug alone increased cytotoxicity to ~8–10% in the absence of virus infection.

To determine if the increased cytotoxicity in SK-N-AS cells correlated with caspase activation, Caspase-Glo Assays were performed at 20 hpi to measure functional levels of effector caspase-3/7. A pan-caspase inhibitor Z-VAD-FMK was added to demonstrate selectivity in the assay. Caspase levels were expressed as fold-over corresponding mock-infected, control samples. Mock-infected cells had low baseline levels of caspase-3/7 activity that were not increased substantially with drug treatment (Fig. 3b). Caspase-3/7 activity was induced in P/V infected cells by ~four-fold irrespective of pre-treatment with either DMSO or 5-azacytidine, and these levels were decreased by addition of Z-VAD-FMK. A similar profile of increased caspase-8 (Fig. 3c) and -9 (Fig. 3d) activity for virus-infected samples was seen for both DMSO and 5-azacytidine pretreatment.

The above in-vitro data indicate that caspases are activated in P/V virus-infected cells, but they did not demonstrate functional roles in mediating cell death. To address this, we tested the hypothesis that cell death observed with combination treatment of 5-azacytidine and P/V virus infection is dependent on caspase activation. SK-N-AS NLR cells were pretreated with either DMSO or 5 μM 5-azacytidine overnight, followed by P/V virus infection at MOI of 10 PFU/cell. Cells were supplemented with DMSO or 5 μM 5-azacytidine and cultured in the presence or absence of Z-VAD-FMK. ROC was recorded every 6 h on the IncuCyte. As shown in Fig. 4a, mock-infected cells continued to proliferate and Z-VAD-FMK had no effect on ROC over time. There was a loss of ROC in mock-infected cells treated with 5-azacytidine, and the addition of Z-VAD-FMK increased ROC by ~30–40%, at later times points (compare blue vs red curves, Fig. 4b). These data indicate that the loss of viability of mock-infected cells by drug treatment is largely caspase-dependent.

In Fig. 4c, the curves for loss of ROC show minimal differences for infected cells with or without the addition of Z-VAD-FMK. The largest effect was seen with cells that underwent combination treatment of 5-azacytidine and P/V virus infection (Fig. 4d), where the addition of Z-VAD-FMK extended the time to reach 50% of time 0 from ~33 h seen with 5-azacytidine plus P/V virus infection (blue curve) to 63 h (red curve).

Taken together, these data indicate that combination treatment of 5-azacytidine and P/V virus infection results in enhanced cytotoxicity. Additionally, P/V infected cells that are treated with DMSO or 5-azacytidine show elevated levels of caspase activation, but the kinetics of killing are not substantially altered by the addition of Z-VAD-FMK in cells infected with P/V virus alone; however, the addition of Z-VAD-FMK had a major effect on the kinetics of killing for cells treated with 5-azacytidine and infected with P/V virus.

Fig. 3

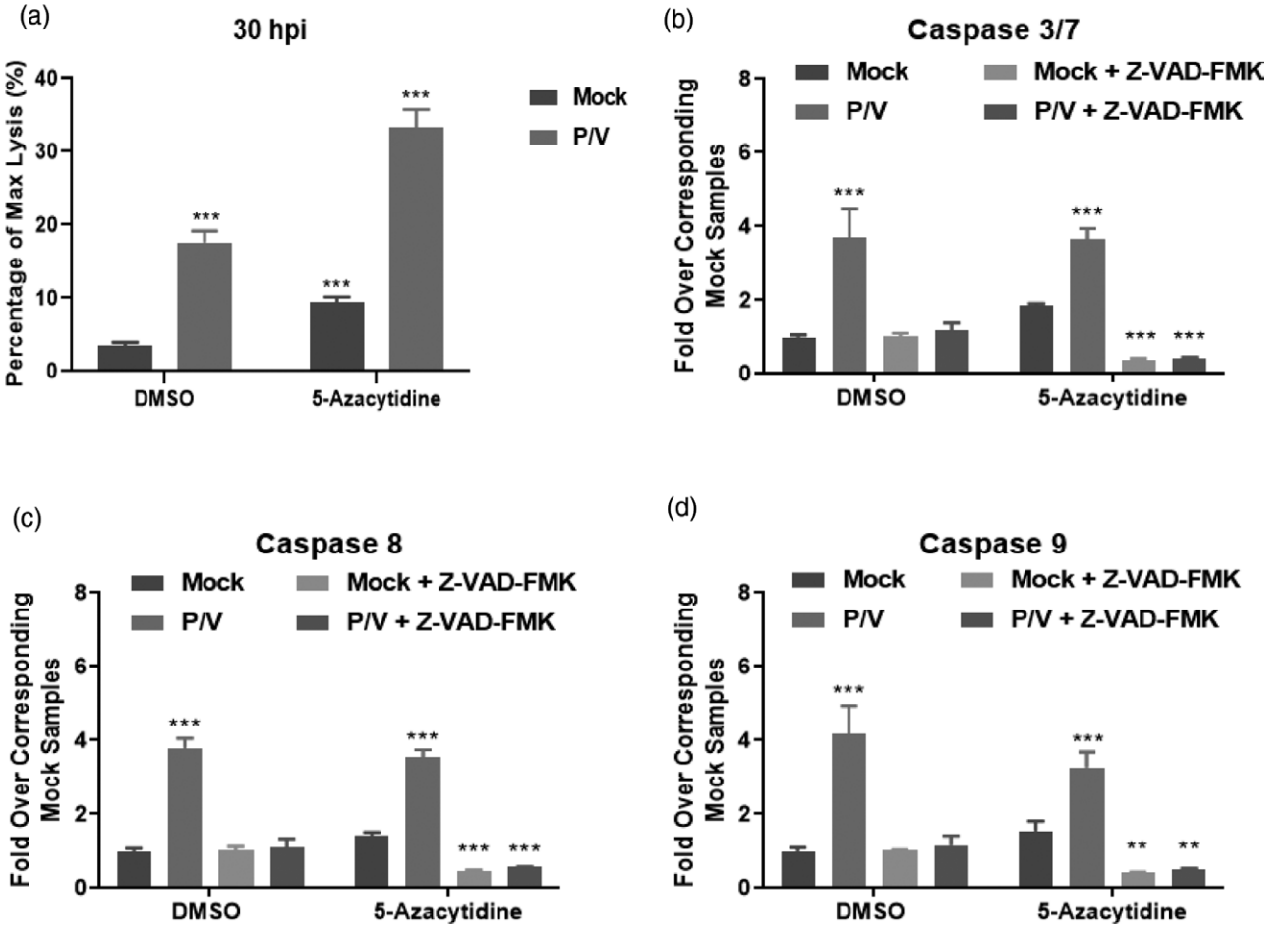

Combination treatment of 5-azacytidine and P/V virus infection induces cell death and caspase activation in neuroblastoma cells. SK-N-AS cells were pretreated with either DMSO or 5 μM 5-azacytidine for ~19 h. Cells were mock-infected or infected with P/V virus at MOI 10 PFU/cell and were then cultured with either DMSO or 5 μM 5-azacytidine. Cytotoxicity was measured using CytoTox-Glo assay at (a) 30 hpi as described in Materials and Methods. Alternatively, samples were assayed for (b) caspase-3/7, (c) caspase-8, and (d) caspase-9 activity by Caspase-Glo Assays at 20 hpi. Samples labelled Z-VAD-FMK are from cells incubated with the pan-caspase inhibitor prior to performing the assay. ** and *** indicate *P* values of <0.002 and <0.001 respectively, when comparing mock-infected samples to corresponding samples within DMSO or 5-azacytidine-treated groups. DMSO, dimethyl sulfoxide; hpi, hours post-infection; MOI, multiplicity of infection; P/V virus, Parainfluenza virus 5.

Pretreatment with 5-azacytidine of Parainfluenza virus 5-infected neuroblastoma cells reduces viral gene expression and growth

The increased cell death observed with the combination of 5-azacytidine and P/V virus infection raised the hypothesis that 5-azacytidine pretreatment enhanced P/V virus replication and growth. To test this, SK-N-AS cells were pretreated with either DMSO or 5 μM 5-azacytidine overnight and then mock-infected or infected with the P/V virus at increasing MOIs of 0.1, 1, and 10 PFU/cell. At 24 hpi, bright field and fluorescence images were taken to measure the expression of GFP, which is encoded within the viral genome, and flow cytometry was performed to quantify the percentage of GFP+ cells. An MOI-dependent increase in the number of GFP+ cells was observed in control P/V virus-infected cells, whereas treatment with 5-azacytidine reduced the overall level of GFP expression in the cell population (Fig. 5a). At an MOI of 10 PFU/cell, ~70% of the DMSO control cells were GFP+, while 5-azacytidine treatment reduced this to ~40% (Fig. 5b). This was also reflected in the MFI of the infected cell population (indicated in parenthesis in Fig. 5b), where a decrease in MFI was observed with 5-azacytidine treatment compared to DMSO control. Viral titres (PFU/ml) from DMSO-treated and infected cells showed a time-dependent increase to ~7 logs at 24 hpi, while 5-azacytidine treatment resulted in ~1.5 logs lower titre (Fig. 5c).

These data indicate that 5-azacytidine treatment reduced viral gene expression and growth within the infected population, inconsistent with the hypothesis that enhanced killing was due to increased virus replication.

Fig. 4

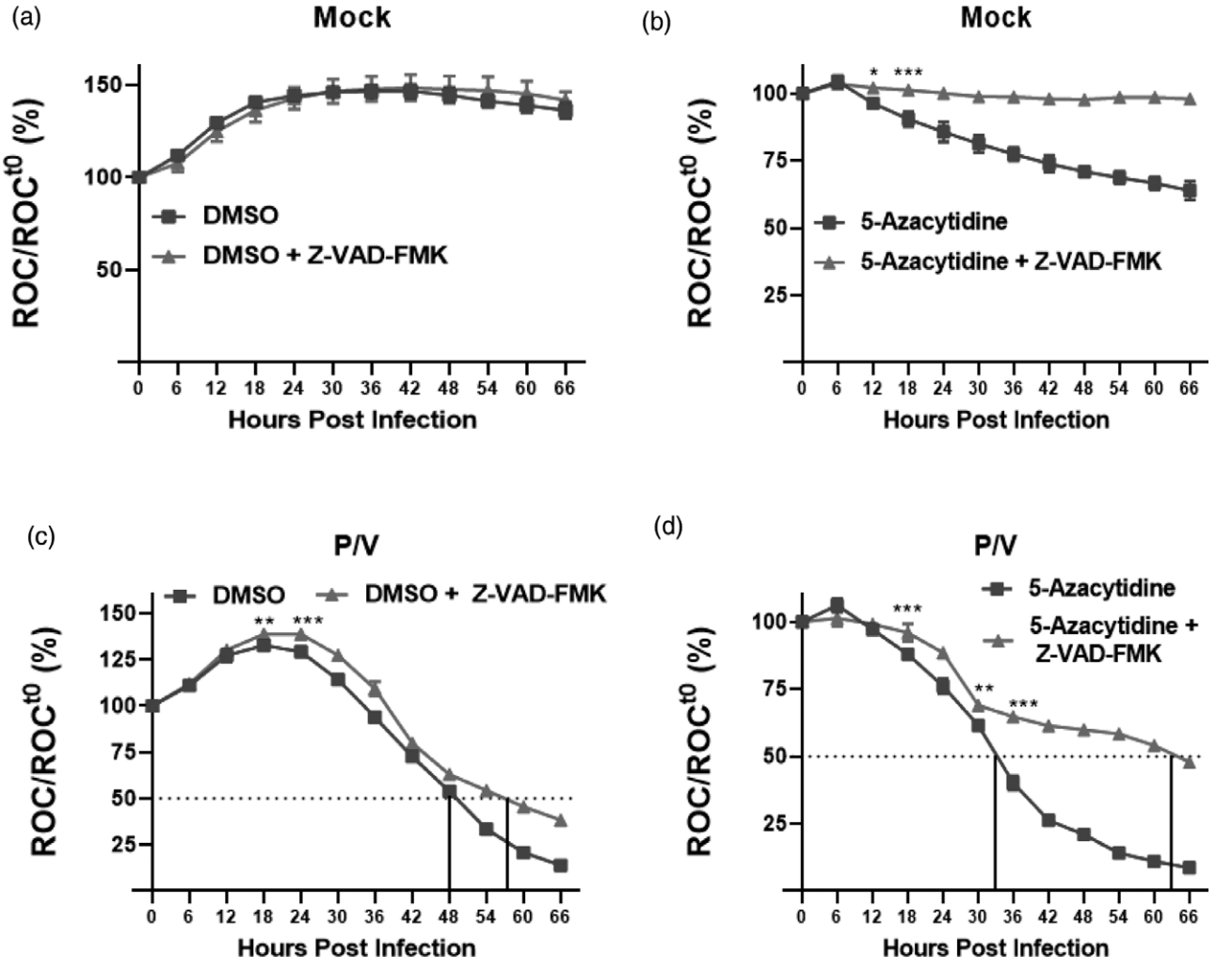

Pan-caspase inhibitor Z-VAD-FMK reduces cell death in neuroblastoma cells largely induced by 5-azacytidine but minimally by P/V virus infection. SK-N-AS NLR cells were pretreated with either (a, c) DMSO or (b, d) 5 μM 5-azacytidine for ~19 h. Cells were (a and b) mock-infected or (c and d) infected with P/V virus at MOI 10 PFU/cell and cultured with the indicated drug, in the presence or absence of 20 μg/ml Z-VAD-FMK. ROC per well was calculated and normalized to ROC at time 0 (ROC^{t0}) when the infection was performed (as described in Fig. 1). Values were expressed as percentage of time 0 and are the mean of three replicates with error bars representing SD. *, **, and *** indicate when *P* values of <0.033, <0.002, and 0.001, respectively, and first begin when comparing virus-infected to mock-infected samples, and this statistical significance extends until a new significance is achieved at later timepoints. DMSO, dimethyl sulfoxide; MOI, multiplicity of infection; NLR, Nuc-Light-Red; P/V virus, Parainfluenza virus 5; ROC, red object count.

Anti-viral gene expression is upregulated by combined treatment of neuroblastoma cells with 5-azacytidine and Parainfluenza virus 5 infection

Given that the P/V virus is a potent inducer of IFN-β [19], we tested the hypothesis that reduced viral gene expression and growth mediated by 5-azacytidine treatment was due to enhanced IFN-β expression. SK-N-AS cells were treated with DMSO or 5 μM 5-azacytidine overnight, and either mock-infected or infected with P/V virus at an MOI of 10 PFU/cell. Total RNA was isolated at 16 and 24 hpi, and *IFN-β* gene expression was evaluated. At 16 hpi, there was a ~15-fold upregulation in *IFN-β* gene expression with both mock- and P/V-infected cells pretreated with 5-azacytidine (Fig. 6a). At 24 hpi, *IFN-β* gene expression was increased by ~150-fold in 5-azacytidine treated and P/V infected cells (Fig. 6b).

We extended our studies to evaluate if 5-azacytidine treatment altered the expression of IFN-I stimulated genes (ISG), including the expression of ISG *OAS2*, a key ISG implicated in P/V virus infection [23]. There was a ~10–15-fold upregulation of *OAS2* at 16 hpi in both mock- and P/V-infected cells that were pretreated with 5-azacytidine (Fig. 6c). At 24 hpi, this was further enhanced to ~50-fold *OAS2* gene expression for virus-infected cells pretreated with 5-azacytidine (Fig. 6d).

Fig. 5

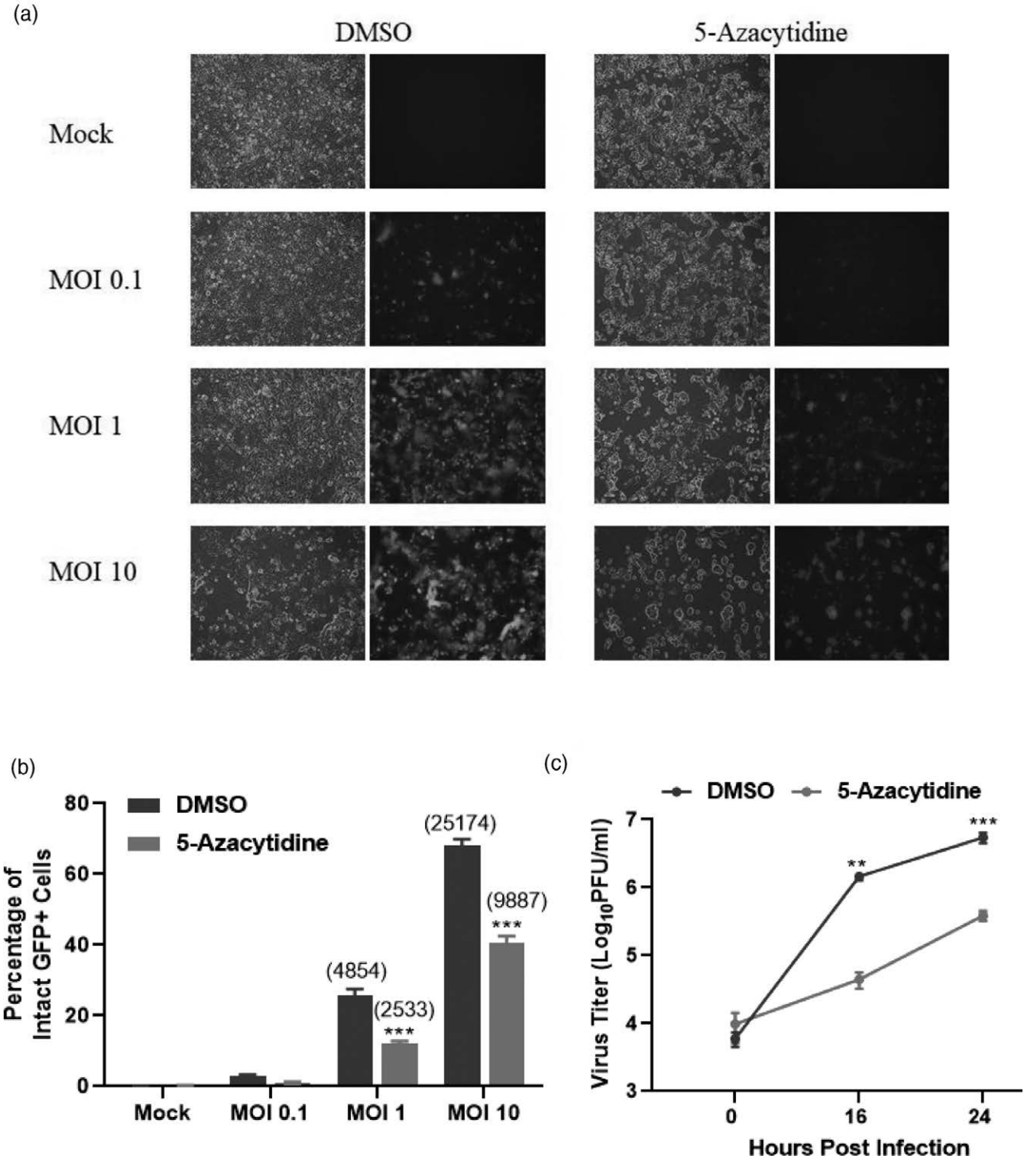

Pretreatment of neuroblastoma cells with 5-azacytidine reduces virus gene expression and progeny virus production. SK-N-AS cells were pretreated with DMSO or 5 μM 5-azacytidine for ~19 h. Cells were either mock-infected or infected with P/V virus at MOI of 0.1, 1, and 10 PFU/cell and cultured with the indicated drug concentration. At 24 hpi, (a) bright field and fluorescence images were captured and (b) the percentage of infected GFP+ cells was quantified by flow cytometry. Mean fluorescence intensity (MFI) for samples is indicated in parentheses. Media from infected cells was collected at 0, 16, and 24 hpi, and plaque assays were performed to quantify (c) infectious virus units. Viral titres were normalized to 10^6 cells and expressed as PFU/ml in the logarithmic scale. Values are the mean of three samples, with error bars representing SD. ** and *** indicate *P* values of <0.002 and <0.001 when comparing to DMSO control and drug-treated samples. DMSO, dimethyl sulfoxide; GFP, green fluorescence protein; hpi, hours post-infection; MOI, multiplicity of infection; P/V virus, Parainfluenza virus 5.

Fig. 6

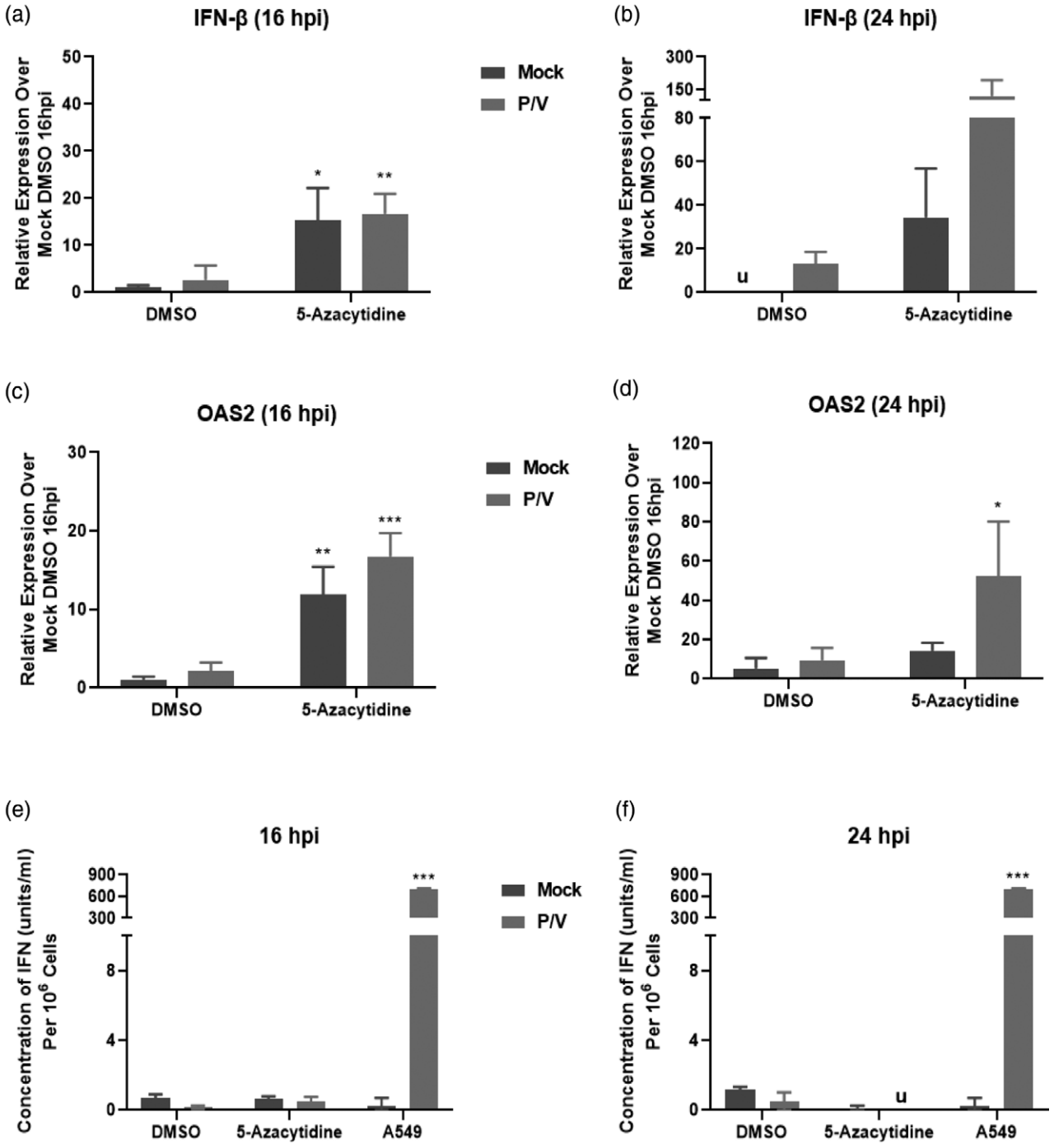

Combination treatment of neuroblastoma cells with 5-azacytidine and P/V virus infection increases expression of antiviral genes. SK-N-AS cells were pretreated with DMSO or 5 μM 5-azacytidine for ~19 h and then mock-infected or infected with P/V virus at MOI of 10 PFU/cell. Cells were then cultured with the indicated drug concentration. Total RNA was isolated at (a, c) 16 or (b, d) 24 hpi to determine levels of (a and b) *IFN-β* and (c and d) *OAS2* using quantitative real-time PCR. Media was also collected at (e) 16 and (f) 24 hpi and biological levels of IFN-I were quantified using a functional detection assay, as described in the Materials and Methods. *, **, and *** indicate *P* values of <0.033, <0.002, and <0.001 when comparing DMSO-treated and mock-infected cells to other samples. 'u' in (b, f) denote undetectable levels of IFN-I. DMSO, dimethyl sulfoxide; hpi, hours post-infection; IFN-I, type I interferon; MOI, multiplicity of infection; P/V virus, Parainfluenza virus 5.

To determine if functional IFN-I was secreted from the cells, a bioassay was performed on media samples collected at 16 and 24 hpi. As shown in Fig. 6e and f, minimal or undetectable (u) amounts of IFN-I were detected, and this was similar to that of the negative control of mock-infected A549 cells. In contrast, the positive control of

Fig. 7

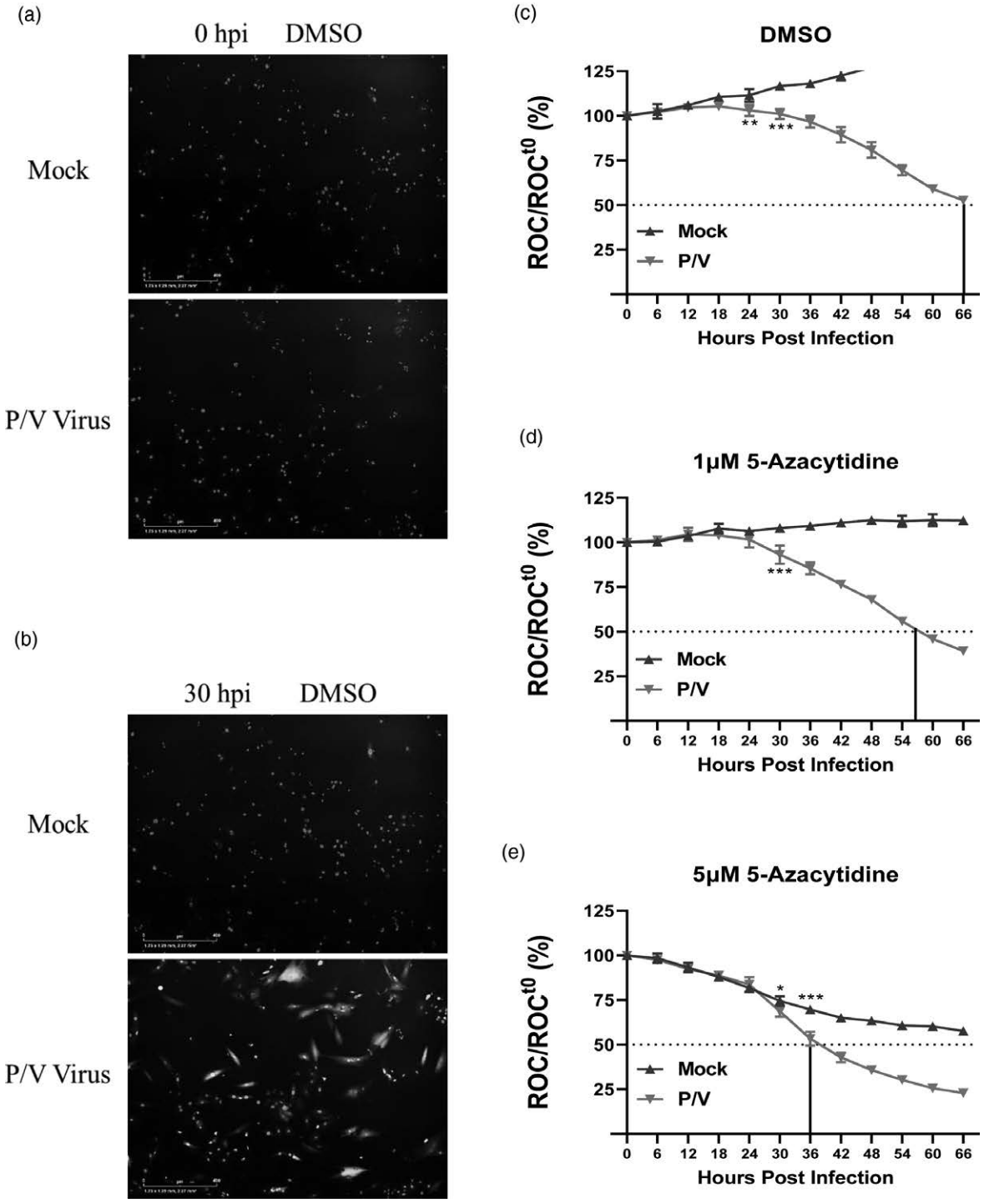

Enhanced killing of SK-N-SH cells by combination treatment with 5-azacytidine and P/V virus infection. SK-N-SH NLR cells were pretreated with either (c) DMSO, or with (d and e respectively) 1 or 5 μM 5-azacytidine for ~19 h. Cells were mock-infected or infected with P/V virus at an MOI of 10 PFU/cell and cultured in the presence of indicated drug concentration. (a and b) show representative fluorescence images taken by the IncuCyte detector at 0 and 30 hpi respectively ROC per well was normalized to ROC at time 0 (ROC^{t0}) as described in Fig. 1. Values were expressed as percentage of time 0 and are the mean of three replicates with error bars representing SD. *, **, and *** indicate when *P* values of <0.033, <0.002, and 0.001 first begin when comparing virus-infected to mock-infected samples, and this statistical significance extends until a new significance is achieved at later timepoints. DMSO, dimethyl sulfoxide; hpi, hours post-infection; MOI, multiplicity of infection; NLR, Nuc-Light-Red; P/V virus, Parainfluenza virus 5; ROC, red object count.

media from P/V infected A549 cells yielded ~900 units/ml of IFN-I levels.

Together, these data indicate that 5-azacytidine treatment increased gene expression of key antiviral genes, *IFN-β* and *OAS2* even in the absence of virus infection, and this was further increased at late times post-infection with P/V virus; however, no biologically active IFN-I was detected from SK-N-AS cells, suggesting that antiviral gene expression is induced in an IFN-independent mechanism.

Combination treatment of 5-azacytidine and Parainfluenza virus 5 infection results in dose-dependent enhanced cell killing in additional neuroblastoma cell line

We extended our analysis to SK-N-SH cells, an additional neuroblastoma cell line. SK-N-SH NLR cells were pretreated with DMSO or increasing doses of 5-azacytidine overnight, followed by mock infection or P/V virus infection. Representative images of cells captured at 0 (Fig. 7a) and 30 hpi (Fig. 7b) after P/V virus infection show red nuclei (ROC) in the SK-N-SH NLR cells and 30 hpi images additionally show GFP expressed by P/V virus infection, indicating that the cell population is susceptible to infection.

DMSO-treated and P/V virus-infected cells show a reduction in ROC, reaching 50% of time 0 by ~66 hpi (Fig. 7c). When pretreated with 5-azacytidine, mock-infected cells showed a dose-dependent decrease in ROC (blue curves, Fig. 7d and e). By contrast, P/V virus-infected cells pretreated with 1 and 5 μM 5-azacytidine (red curves, Fig. 7d and e) had enhanced loss of ROC reaching 50% of time 0 at ~56 and 36 hpi, respectively. Together, these data demonstrate that 5-azacytidine treatment leads to increased P/V virus-mediated killing in an additional neuroblastoma cell line.

Discussion

Previous studies have indicated that treatment of lung carcinoma cells with HDAC inhibitors enhanced virus-mediated killing by P/V virus, a cytoplasmic-replicating negative sense RNA virus [23]. This led us to test a more general hypothesis that treatment with synthetic epigenetic modulators that act through a different mechanism would also enhance P/V virus-mediated killing. We chose to test this hypothesis using neuroblastoma cells, which have been shown to respond to DNMT modulation [3]. Here, we have shown that pretreatment with the DNMTi nucleoside analog 5-azacytidine sensitizes SK-N-AS neuroblastoma cells to enhanced P/V virus-mediated death in a dose- and MOI-dependent manner. Interestingly, pretreatment with 5-azacytidine resulted in reduced virus growth and spread kinetics, which correlated with enhanced gene expression of antiviral genes such as *IFN-β* and *OAS2*. Together, our data support the general hypothesis that different classes of s epigenetic modulators, such as HDAC and DNMT inhibitors, can enhance the oncolytic P/V virus killing of cancer cells.

How do inhibitors of epigenetic-modulating proteins such as HDAC and DNMT which function in the cell nucleus augment the ability of a cytoplasmic-replicating RNA virus to kill cancer cells? Cell death for a particular cell type is balanced by the combination of death-activating proteins (e.g. caspases) and the presence of death-inhibiting components such as inhibitors of apoptosis proteins (IAPs) [28]. We have previously shown using chemical inhibitors that the viability of P/V virus-infected lung cancer cells is highly dependent on the IAPs, XIAP, and Survivin [29]. It is possible that inhibition of DNMT activity in 5-azacytidine-treated neuroblastoma cells shifts this balance to favour death-inducing pathways by decreasing IAP expression or activity.

As an alternative mechanism for enhanced killing, P/V infection and 5-azacytidine treatment of SK-N-AS neuroblastoma cells could activate independent cell death pathways which, when combined, lead to higher cell killing than the corresponding single treatments. Although caspase -8, -9, and -3/7 were activated for cells infected with P/V virus only and also in cells treated together with 5-azacytidine and P/V virus (Fig. 3b–d), it is important to note that caspase activation does not demonstrate the direct cause of cell death. As evidence of this, the addition of the pan-caspase inhibitor Z-VAD-FMK (Fig. 4) to mock-infected cells largely restored the loss of cell viability observed with 5-azacytidine treatment. By contrast, the loss of viability in P/V virus-infected SK-N-AS cells was largely unaltered by Z-VAD-FMK. Most importantly, the addition of Z-VAD-FMK had a large effect on the viability of cells receiving the combined treatment of 5-azacytidine and P/V virus. These data indicate that caspase-dependent and -independent cell death pathways are induced by 5-azacytidine treatment and P/V virus infection respectively, and a dominant caspase-dependent killing for the combination treatment is observed.

We initially hypothesized that enhanced P/V virus-mediated death observed with 5-azacytidine pretreatment was due to an increase in viral gene expression or virus infectivity within the tumour cell population. Contrary to this hypothesis, 5-azacytidine treatment reduced P/V virus spread and production of progeny virus. The incorporation of 5-azacytidine into cellular RNA has been shown to interfere with tRNA activity, thereby leading to disruption in ribosomal processing and protein synthesis [30–32]. We have previously shown that the P/V virus is capable of shutting off the host and viral translation through the activation of PKR [21]. Thus, it is possible that the dampening of protein translation by both 5-azacytidine and the P/V virus infection could contribute towards reduced viral gene expression and growth, as well as the lack of secreted IFN-I protein.

The canonical IFN-I response to infection is initiated by the activation of transcription factors such as interferon regulatory elements (IRFs), IRF-1 and IRF-3, which drive IFN-I secretion [18]. Secreted IFN-I then binds in an autocrine or paracrine manner to its receptor (IFNAR) to trigger the STAT1-dependent signalling phase, to induce ISGs that create an antiviral state. Alternatively, some IRFs, such as IRF-1, can directly activate ISG expression independent of IFN-I secretion [33]. This could also explain the stimulation of ISG *OAS2* despite the detection of functional and secreted IFN-I.

Interestingly, a prior study showed that treatment with 5-azacytidine led to the generation of cellular dsRNA, which is transcribed from hypomethylated repetitive elements within the host cell chromosome [34]. Accumulation of self dsRNA triggered the IFN-I response and subsequently ISG expression, particularly of OAS proteins which activated latent enzyme RNase L. RNase L is capable of cleaving cellular and viral RNAs, therefore interfering with the viral replication cycle and inducing apoptosis [18,35]. Studies have also shown that the P/V virus generates enhanced levels of dsRNA during its viral replication cycle [21,23]. Together, this raises the hypothesis that overall enhanced virus-mediated death of 5-azacytidine pretreated neuroblastoma cells is induced through dsRNA production and downstream signalling by both drug treatment and virus infection. Future studies will investigate the levels of dsRNA produced in response to 5-azacytidine pretreatment and P/V virus infection in neuroblastoma cells.

In summary, this study outlines the importance of investigating multiple therapeutic approaches to be used in combination, particularly for high-risk neuroblastoma tumours that respond poorly to traditional therapeutics. The results show that the type of DNMT modulator (5-azacytidine) and virus (cytoplasmic-replicating RNA virus) combination should be assessed for cell killing, but also for the effect of these therapeutics on host death pathways and immune responses.

Acknowledgements

We thank members of the Parks lab for their scientific input and Maria Mayol for excellent technical assistance. This study was supported in part by a grant from the Florida Department of Health Live Like Bella number 22L05.

Conflicts of interest

There are no conflicts of interest.

References

1 Matthay KK, Maris JM, Schleiermacher G, Nakagawara A, Mackall CL, Diller L, *et al*. Neuroblastoma. *Nat Rev Dis Primers* 2016; **2**:16078.
2 Maris JM, Hogarty MD, Bagatell R, Cohn SLN. Neuroblastoma. *Lancet* 2007; **369**:2106–2120.
3 Jubierre L, Jiménez C, Rovira E, Soriano A, Sábado C, Gros L, *et al*. Targeting of epigenetic regulators in neuroblastoma. *Exp Mol Med* 2018; **50**:1–12.
4 Qiu YY, Mirkin BL, Dwivedi RS. Inhibition of DNA methyltransferase reverses cisplatin induced drug resistance in murine neuroblastoma cells. *Cancer Detect Prev* 2005; **29**:456–463.
5 Christman JK. 5-Azacytidine and 5-aza-2'-deoxycytidine as inhibitors of DNA methylation: mechanistic studies and their implications for cancer therapy. *Oncogene* 2002; **21**:5483–5495.
6 Sorm F, Píškala A, Cihák A, Veselý J. 5-Azacytidine, a new, highly effective cancerostatic. *Experientia* 1964; **20**:202–203.
7 Fenaux P, Mufti GJ, Hellstrom-Lindberg E, Santini V, Finelli C, Giagounidis A, *et al*.; International Vidaza High-Risk MDS Survival Study Group. Efficacy of azacitidine compared with that of conventional care regimens in the treatment of higher-risk myelodysplastic syndromes: a randomised, open-label, phase III study. *Lancet Oncol* 2009; **10**:223–232.
8 Russell SJ, Peng KW, Bell JC. Oncolytic virotherapy. *Nat Biotechnol* 2012; **30**:658–670.
9 Fukuhara H, Ino Y, Todo T. Oncolytic virus therapy: a new era of cancer treatment at dawn. *Cancer Sci* 2016; **107**:1373–1379.
10 Andtbacka RH, Kaufman HL, Collichio F, Amatruda T, Senzer N, Chesney J, *et al*. Talimogene laherparepvec improves durable response rate in patients with advanced melanoma. *J Clin Oncol* 2015; **33**:2780–2788.
11 Liu BL, Robinson M, Han ZQ, Branston RH, English C, Reay P, *et al*. ICP34.5 deleted herpes simplex virus with enhanced oncolytic, immune stimulating, and anti-tumour properties. *Gene Ther* 2003; **10**:292–303.
12 Asada T. Treatment of human cancer with mumps virus. *Cancer* 1974; **34**:1907–1928.
13 Fiola C, Peeters B, Fournier P, Arnold A, Bucur M, Schirrmacher V. Tumor selective replication of Newcastle disease virus: association with defects of tumor cells in antiviral defence. *Int J Cancer* 2006; **119**:328–338.
14 Pecora AL, Rizvi N, Cohen GI, Meropol NJ, Sterman D, Marshall JL, *et al*. Phase I trial of intravenous administration of PV701, an oncolytic virus, in patients with advanced solid cancers. *J Clin Oncol* 2002; **20**:2251–2266.
15 Myers R, Greiner S, Harvey M, Soeffker D, Frenzke M, Abraham K, *et al*. Oncolytic activities of approved mumps and measles vaccines for therapy of ovarian cancer. *Cancer Gene Ther* 2005; **12**:593–599.
16 Peng KW, TenEyck CJ, Galanis E, Kalli KR, Hartmann LC, Russell SJ. Intraperitoneal therapy of ovarian cancer using an engineered measles virus. *Cancer Res* 2002; **62**:4656–4662.
17 Galanis E, Hartmann LC, Cliby WA, Long HJ, Peethambaram PP, Barrette BA, *et al*. Phase I trial of intraperitoneal administration of an oncolytic measles virus strain engineered to express carcinoembryonic antigen for recurrent ovarian cancer. *Cancer Res* 2010; **70**(3):875–882.
18 Randall RE, Goodbourn S. Interferons and viruses: an interplay between induction, signalling, antiviral responses and virus countermeasures. *J Gen Virol* 2008; **89**(Pt 1):1–47.
19 Wansley EK, Parks GD. Naturally occurring substitutions in the P/V gene convert the noncytopathic paramyxovirus simian virus 5 into a virus that induces alpha/beta interferon synthesis and cell death. *J Virol* 2002; **76**:10109–10121.
20 Wansley EK, Grayson JM, Parks GD. Apoptosis induction and interferon signaling but not IFN-beta promoter induction by an SV5 P/V mutant are rescued by coinfection with wild-type SV5. *Virology* 2003; **316**:41–54.
21 Gainey MD, Dillon PJ, Clark KM, Manuse MJ, Parks GD. Paramyxovirus-induced shutoff of host and viral protein synthesis: role of the P and V proteins in limiting PKR activation. *J Virol* 2008; **82**:828–839.
22 Gainey MD, Manuse MJ, Parks GD. A hyperfusogenic F protein enhances the oncolytic potency of a paramyxovirus simian virus 5 P/V mutant without compromising sensitivity to type I interferon. *J Virol* 2008; **82**:9369–9380.
23 Fox CR, Parks GD. Histone deacetylase inhibitors enhance cell killing and block interferon-beta synthesis elicited by infection with an oncolytic parainfluenza virus. *Viruses* 2019; **11**:431.
24 Kedarinath K, Parks GD. Differential in vitro growth and cell killing of cancer versus benign prostate cells by oncolytic parainfluenza virus. *Pathogens* 2022; **11**:493.
25 Kedarinath K, Fox CR, Crowgey E, Mazar J, Phelan P, Westmoreland TJ, *et al*. CD24 expression dampens the basal antiviral state in human neuroblastoma cells and enhances permissivity to zika virus infection. *Viruses* 2022; **14**:1735.
26 Varudkar N, Oyer JL, Copik A, Parks GD. Oncolytic parainfluenza virus combines with NK cells to mediate killing of infected and non-infected lung cancer cells within 3D spheroids: role of type I and type III interferon signaling. *J ImmunoTher Cancer* 2021; **9**:e002373.

27 Fox CR, Parks GD. Complement inhibitors vitronectin and clusterin are recruited from human serum to the surface of coronavirus OC43-infected lung cells through antibody-dependent mechanisms. *Viruses* 2021; **14**:29.
28 Silke J, Meier P. Inhibitor of apoptosis (IAP) proteins-modulators of cell death and inflammation. *Cold Spring Harb Perspect Biol* 2013; **5**:1–19.
29 Fox CR, Parks GD. Parainfluenza virus infection sensitizes cancer cells to DNA-damaging agents: implications for oncolytic virus therapy. *J Virol* 2018; **92**. doi: 10.1128/JVI.01948-17.
30 Lu LJ, Randerath K. Mechanism of 5-azacytidine-induced transfer RNA cytosine-5-methyltransferase deficiency. *Cancer Res* 1980; **40**(8 Pt 1):2701–2705.
31 Avramis VI, Powell WC, Mecum RA. Cellular metabolism of 5,6-dihydro-5-azacytidine and its incorporation into DNA and RNA of human lymphoid cells CEM/O and CEM/dCk(-). *Cancer Chemother Pharmacol* 1989; **24**:155–160.
32 Weiss JW, Pitot HC. Alteration of ribosomal precursor RNA in Novikoff hepatoma cells by 5-azacytidine. Studies on methylation of 45S and 32S RNA. *Arch Biochem Biophys* 1974; **165**:588–596.
33 Panda D, Gjinaj E, Bachu M, Squire E, Novatt H, Ozato K, *et al*. IRF1 maintains optimal constitutive expression of antiviral genes and regulates the early antiviral response. *Front Immunol* 2019; **10**:1019.
34 Banerjee S, Gusho E, Gaughan C, Dong B, Gu X, Holvey-Bates E, *et al*. OAS-RNase L innate immune pathway mediates the cytotoxicity of a DNA-demethylating drug. *Proc Natl Acad Sci U S A* 2019; **116**:5071–5076.
35 Castelli JC, Hassel BA, Wood KA, Li XL, Amemiya K, Dalakas MC, *et al*. A study of the interferon antiviral mechanism: apoptosis activation by the 2-5A system. *J Exp Med* 1997; **186**:967–972.